

Supporting Information

Ultrathin Phyllosilicate Nanosheets as Anode Material with Superior Rate Performance for Lithium Ion Batteries

Xiang-Qian Zhang¹, Wen-Cui Li¹, Bin He¹, Dong Yan¹, Shuang Xu¹, Yuliang Cao², An-Hui Lu*¹

1 School of Chemical Engineering, State Key Laboratory of Fine Chemicals, Dalian University of Technology, Dalian 116024, P. R. China

2 Hubei Key Laboratory of Electrochemical Power Sources, College of Chemistry and Molecular Sciences, Wuhan University, Wuhan, Hubei 430072, P. R. China

*Corresponding Author: An-Hui Lu

E-mail: anhuilu@dlut.edu.cn Phone/Fax number: +86-411-84986112

List of contents:

Scheme S1. Schematic illustration for the growth strategies of nickel silicates on substrate (a) in this work and (b) previous reported work.

Figure S1. (a) STEM image and the linear EDX element distributions of carbon (C) and silicon (Si) of tubular mesoporous carbon/silica composite. (b) N₂ adsorption-desorption isotherm of carbon/silica composite.

Figure S2. HAADF-STEM image of the CNSF and the corresponding EDS mapping of C, Ni, and Si elements.

Figure S3. (a,b) SEM images and (c) EDX mapping of bare NSF.

Figure S4. EDX spectrum of CNSF material. Inset shows the elements ratios.

Figure S5. (a) CV curves and (b) EIS spectra of CNSF.

Figure S6. (a) CV curves and (b) GC profiles of bare NSF.

Figure S7. XRD patterns and electrochemical performance of (a,c) carbon-incorporated manganese silicate (CMnSF) and (b,d) carbon-incorporated copper silicate (CCuSF).

Figure S8. SEM images and EDX mapping of CNSF after cycles.

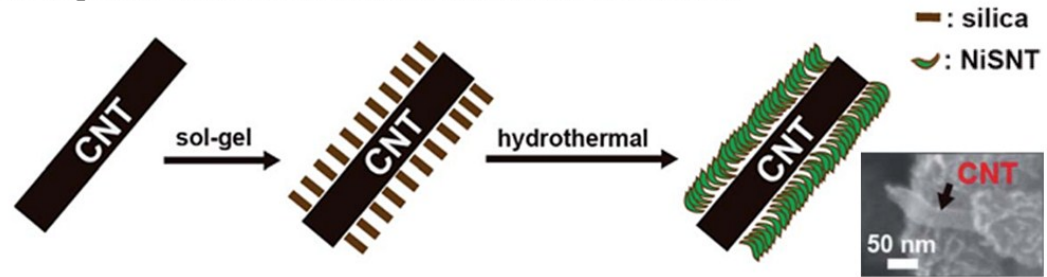
Figure S9. (a). Cycling performance of commercial LiNi_{1/3}Co_{1/3}Mn_{1/3}O₂ (LiNCM) cathode at 0.2 C with corresponding charge/discharge profiles as inset. (b) Rate capacity of LiNCM cathode.

Table S1. The reported performance of nickel silicates anodes for lithium ion batteries and the results in this study.

A: This work



B: Reported work in reference *J. Mater. Chem. A*, 2015, 3, 16551



Scheme S1. Schematic illustration for the growth strategies of nickel silicates on substrate (a) in this work and (b) previous reported work.

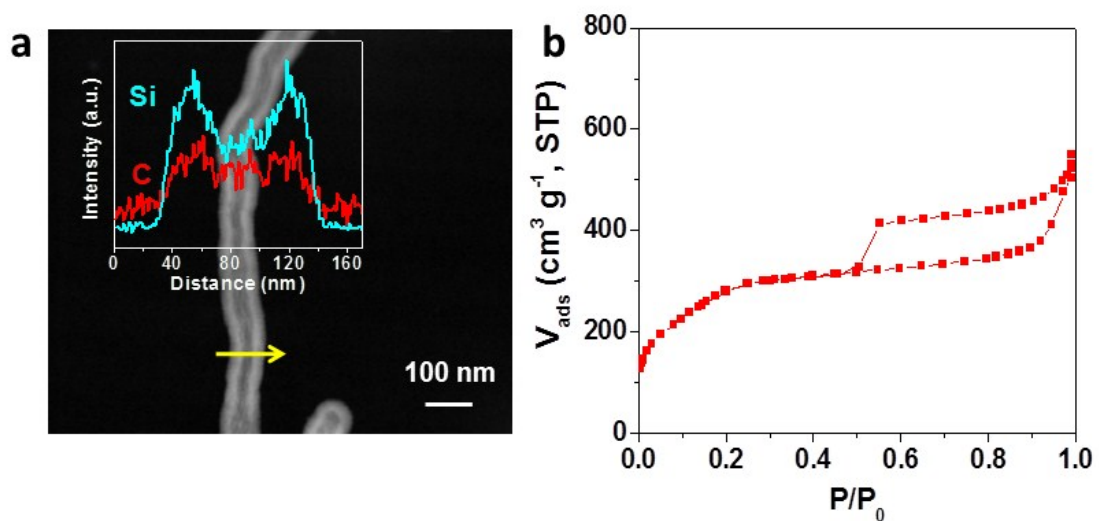


Figure S1. (a) STEM image and the linear EDX element distributions of carbon (C) and silicon (Si) of tubular mesoporous carbon/silica composite. (b) N₂ adsorption-desorption isotherm of carbon/silica composite.

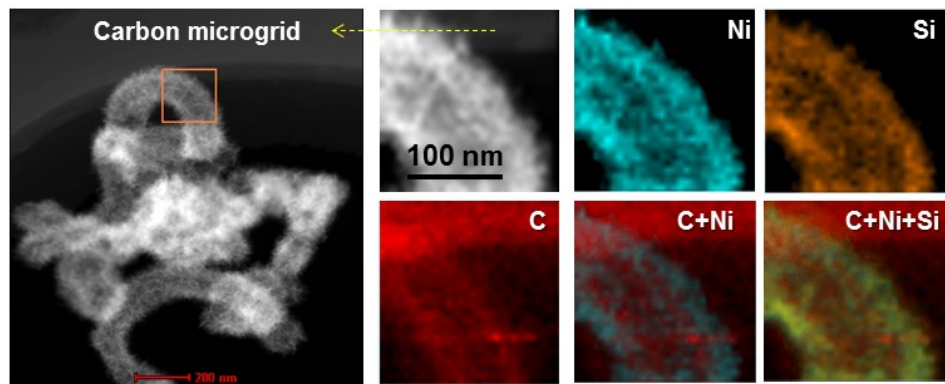


Figure S2. HAADF-STEM image of the CNSF and the corresponding EDS mapping of C, Ni, and Si elements.

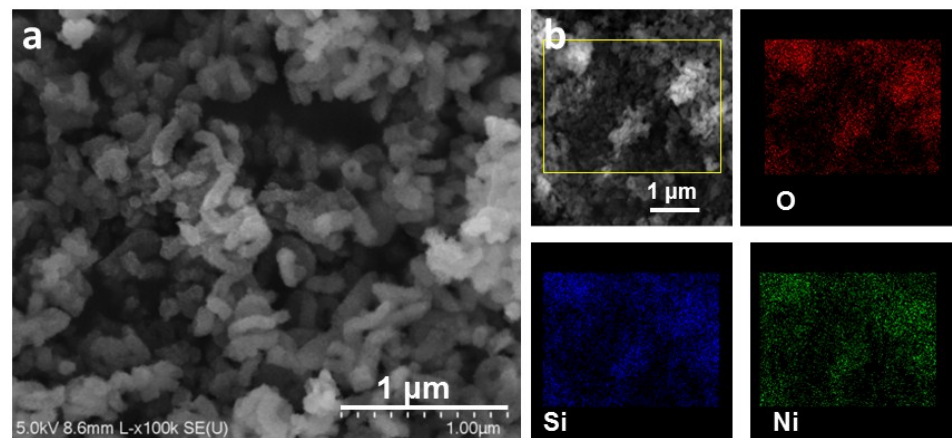


Figure S3. (a) SEM image and (b) EDX mapping of bare NSF.

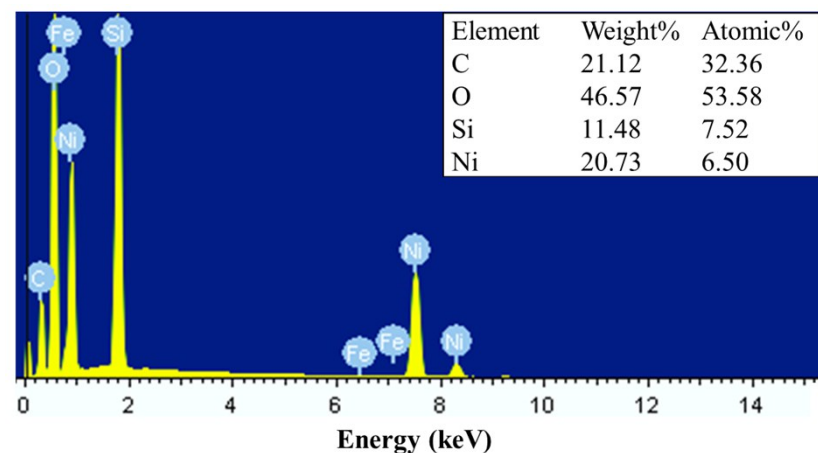


Figure S4. EDX spectrum of CNSF material. Inset shows the elements ratios. Comments: A trace amount of Fe (Fe/Ni weight ratio=0.0048) was present due to the contamination in the product.

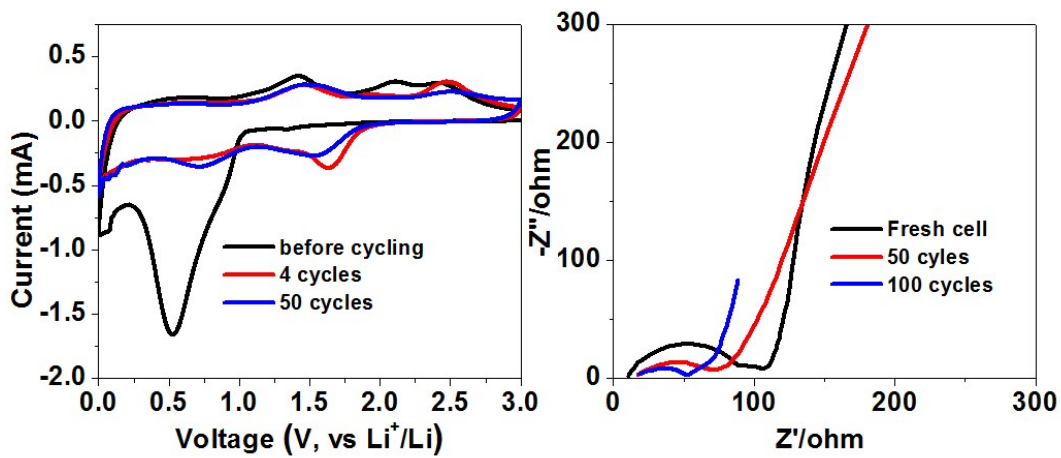


Figure S5. (a) CV curves and (b) EIS spectra of CNSF.

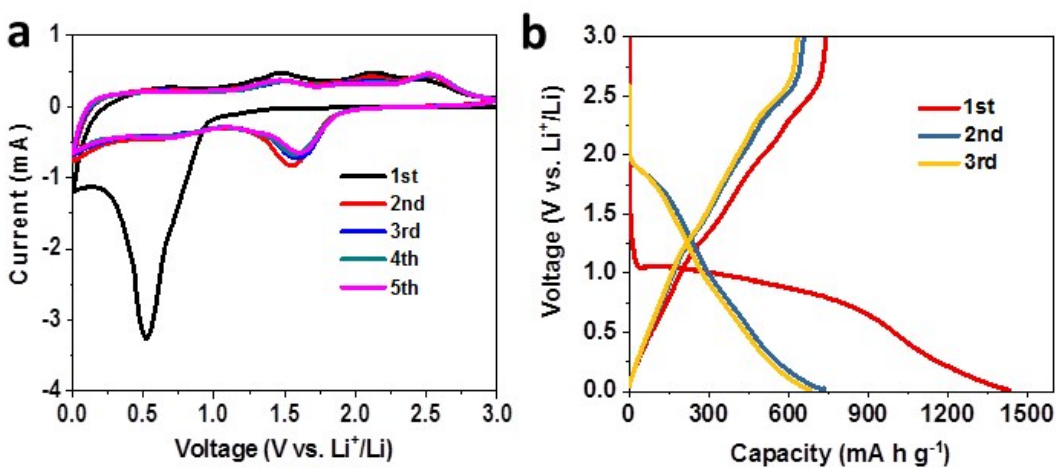


Figure S6. (a) CV curves and (b) GC profiles of bare NSF.

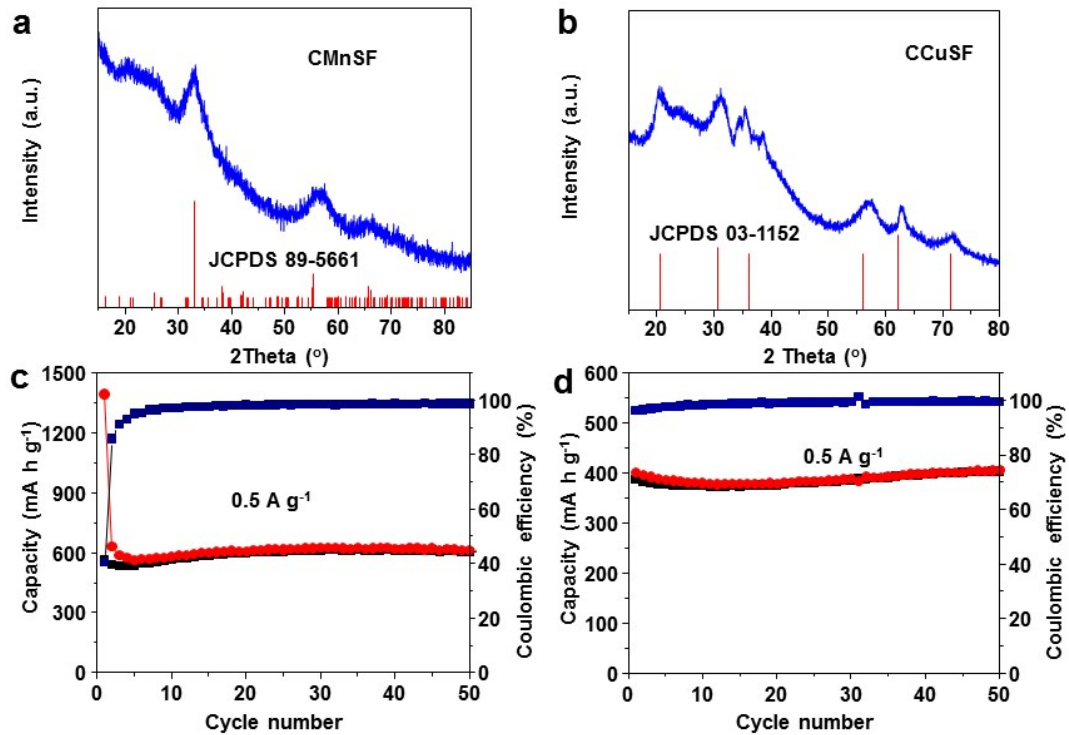


Figure S7. XRD patterns and electrochemical performance of (a,c) carbon-incorporated manganese silicate (CMnSF) and (b,d) carbon-incorporated copper silicate (CCuSF).

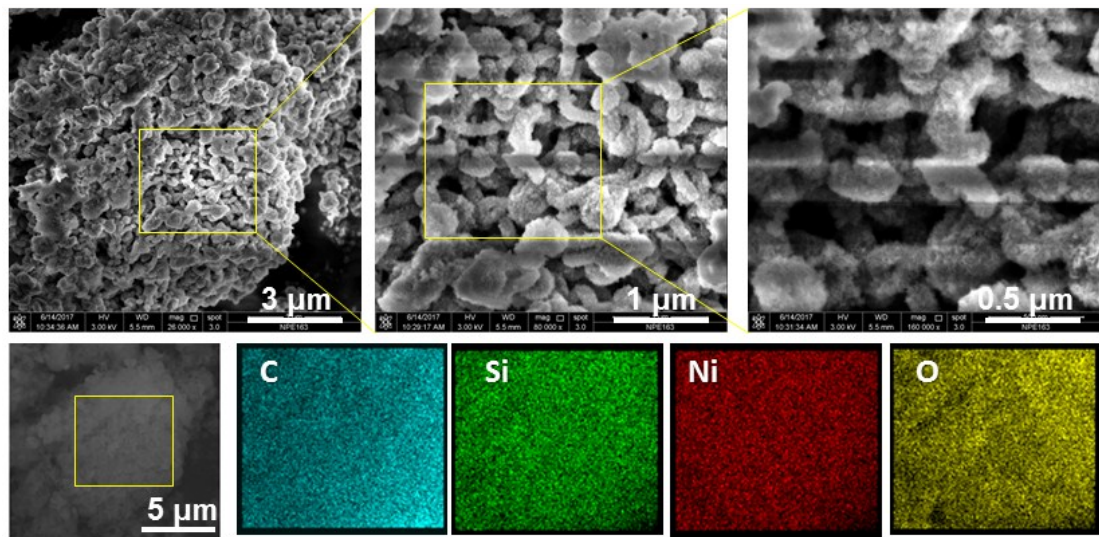


Figure S8. SEM images and EDX mapping of CNSF after cycles.

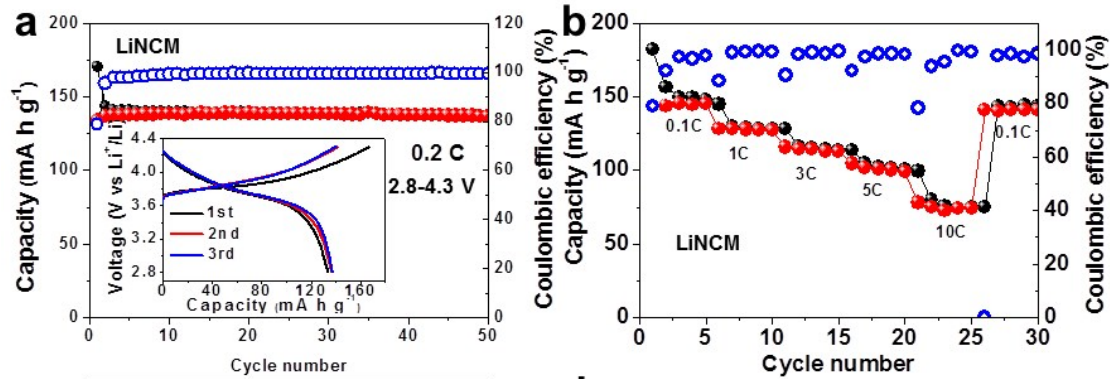


Table S1. The reported performance of nickel silicates anodes for lithium ion batteries and the results in this study.

Samples	Initial coulombic efficiency	Initial charge capacity	Cyclic stability	Rate capability	Ref.
CNSF	70.7%@0.05	1181	585@1.0 (200th)	1145@0.05	
				1107@0.1	
				1017@0.2	This work
				876@0.5	
				730@1.0	
Ni-HNs	42%@0.2 ^a	500 ^a	673.8@0.2 (300th)	540@2.0	
				~700@0.1 ^a	
				550@0.3	1
NiO/NiSiO nanoflowers	46.7%@0.05	672	126 ^b @0.05 (50th)	400@1.0	
				NG ^c	2
Nickel silicate nanoplates on RGO	59%@0.05	730 ^a	797@0.05 (50th)	656@0.1	
				601@0.2	
				534@0.5	3
				484@1.0	
rGO/NiSiO/Ni	NG ^c	698	478@0.02 (60th)	~500@0.05	
				420@0.1	4
rGO/NiSiO	44%@0.02	758	380.5@0.02 (60th)	~400@0.05	
				280@0.1	
CNT@NiSiOx	71.5%@0.05	770	489@0.05 (50th)	387@0.1	
				293@0.2	
				210@0.5	5
				157@1.0	
RGO wrapped NiSiO hollow spheres	66.3%@0.2	1024	400@0.5 (1000th)	592@0.1	
				488@0.2	
				407@0.5	6
				275@1.0	
				143@2.0	
Ni ₃ Si ₂ O ₅ (OH) ₄ nanotube	45.5%@0.02	639	227@0.02 (21th)	NG ^c	
				571@0.05	7
Copper Silicate Hydrate /RGO	45.5%@0.2	1100	747@1.0 (1st) 431@1.0 (2nd) 429@1.0 (800th)	522@0.1	
				460@0.2	8
				398@0.5	
				357@1.0	
cobalt silicate nanobelts@carbon (20.9wt% carbon)	53.3@0.08	620.9	686.4@0.5 (100th) 450@0.5 (1000th)	745@0.1	
				688@0.2	9
				580@0.5	

						478@1.0
						360@2.0
Zn ₂ SiO ₄	urchin-like microspheres	57.5@0.05	532	413@0.05 (20th)	NG	10
fayalite	(a- Fe ₂ SiO ₄)@C	60.6@0.1C	514.5	376.7@1.0C (100th)	514.5@0.1C 465.3@0.2C 428.7@0.5C 412.6@1.0C 384.5@2.0C 372.4@3.0C	11

a, Values estimated from Graph; b, Lithiation capacity; c, Not given

References

- [1] S. -H. Yu, B. Quan, A. Jin, K. -S. Lee, S. H. Kang, K. Kang, Y. Piao, Y. -E. Sung, ACS Appl. Mater. Interfaces 2015, 7, 25725–25732.
- [2] Y. Yang, R. Jin, S. Song, Y. Xing, Mater. Lett. 2013, 93, 5–8.
- [3] Q. -Q. Wang, J. Qu, Y. Liu, C. -X. Gui, S. -M. Hao, Y. Yu, Z. -Z. Yu, Nanoscale 2015, 7, 16805–16811.
- [4] R. Jin, Y. Yang, Y. Li, X. Liu, Y. Xing, S. Song, Z. Shi, Chem. Eur. J. 2015, 21, 9014 – 9017.
- [5] C. -X. Gui, S. -M. Hao, Y. Liu, J. Qu, C. Yang, Y. Yu, Q. -Q. Wang, Z. -Z. Yu, J. Mater. Chem. A 2015, 3, 16551–16559.
- [6] C. Tang, J. Sheng, C. Xu, S. M. B. Khajehbashi, X. Wang, P. Hu, X. Wei, Q. Wei, L. Zhou, L. Mai, J. Mater. Chem. A 2015, 3, 19427–19432.
- [7] Y. Yang, Q. Liang, J. Li, Y. Zhuang, Y. He, B. Bai, X. Wang, Nano Res. 2011, 4(9), 882–890.
- [8] X. Wei, C. Tang, X. Wang, L. Zhou, Q. Wei, M. Yan, J. Sheng, P. Hu, B. Wang, L. Mai, ACS Appl. Mater. Interfaces 2015, 7, 26572–26578.
- [9] W. Cheng, F. Rechberger, G. Ilari, H. Ma, W. -I. Lin, M. Niederberger, Chem. Sci. 2015, 6, 6908–6915.
- [10] S. Zhang, L. Ren, S. Peng, CrystEngComm 2014, 16, 6195–6202.
- [11] Q. Zhang, S. Ge, H. Xue, X. Wang, H. Sun, A. Li, RSC Adv. 2014, 4, 58260–58264.